

Kinetic temperature and pressure of an active Tonks gas

Elijah Schiltz-Rouse,¹ Hyeonjoo Row,^{2,*} and Stewart A. Mallory^{1,†}

¹*Department of Chemistry, The Pennsylvania State University, University Park, Pennsylvania, 16802, USA*

²*Department of Chemical and Biomolecular Engineering, UC Berkeley, Berkeley, CA 94720, USA*

(Dated: January 9, 2024)

Using computer simulation and analytical theory, we study an active analog of the well-known Tonks gas, where active Brownian particles are confined to a periodic one-dimensional (1D) channel. By introducing the notion of a kinetic temperature, we derive an accurate analytical expression for the pressure and clarify the paradoxical behavior where active Brownian particles confined to 1D exhibit anomalous clustering but no motility-induced phase transition. More generally, this work provides a deeper understanding of pressure in active systems as we uncover a unique link between the kinetic temperature and swim pressure valid for active Brownian particles in higher dimensions.

A fundamental model for understanding the behavior of liquids is the one-dimensional (1D) hard rod fluid or Tonks gas [1], where purely-repulsive particles are confined to move in a 1D channel. The statistical mechanics of this system can be solved exactly, and many of its equilibrium properties are derivable in a closed analytical form [1–8]. There is a rich history in statistical physics of studying the Tonks gas and its variations to validate theories and approximation [9–16]. More recently, 1D models have achieved elevated importance as meaningful representations of physical systems, including the single-file diffusion of colloids in microfluidic channels, ion transport across cellular membranes, and the clustering of red blood cells in microcapillary flows [17–25].

Here, we focus on an active variant of the Tonks gas where active Brownian particles are restricted to move in a narrow channel. Active Brownian particles (ABPs) are a popular minimal model for self-propelled particles as their collective behavior captures many of the features exhibited by active suspensions [26–33]. Understanding the active Tonks gas is paramount, as many of the proposed applications of microscopic active matter will operate in highly confined environments. Examples include targeted drug delivery to specific cellular targets [34–36] and the autonomous exploration of porous media [37, 38]. Also, active particles tend to accumulate on surfaces, leading to the formation of 1D boundary layers [39–48].

Surprisingly, there is little work exploring the role of pressure in 1D active systems. Nevertheless, pressure is critical in characterizing the behavior of active systems [49–61], and has aided in explaining a variety of phenomena, including motility-induced phase separation [62–72], active particle motion within vesicles and droplets [73–80] and the dynamics of passive colloidal structures in an active bath [81–99]. In this work, we introduce the concept of a kinetic temperature to aid in deriving an accurate analytical expression for the pressure of an active Tonks gas. Inspiration is taken from the study of granular matter, where a granular temperature can be defined to account for the inelastic nature of collisions [16]. We find excellent agreement between our analytical result and numerical simulation. In addition,

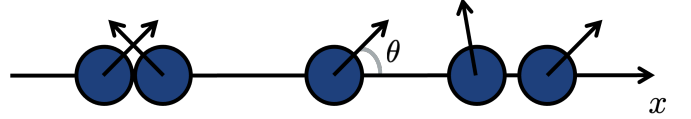


FIG. 1. Schematic of 1D-ABP system. Each purely-repulsive particle moves at a speed $U_a \cos \theta$ while undergoing rotational Brownian motion with reorientation time τ_R .

we derive an exact relation between the kinetic temperature and the so-called swim pressure [52, 65] valid for ABPs in any dimension. To conclude, we explain the unusual clustering observed in 1D active systems and the absence of a motility-induced phase transition.

To model the active Tonks gas or 1D-ABP system, we consider N purely-repulsive active Brownian disks confined to a periodic 1D channel of length L as shown in Fig. 1. An active force $F_a = \gamma U_a \cos \theta$ is applied to each particle where θ is the angle between the positive x -axis and the particle's orientation vector, γ the translation drag coefficient, and U_a the constant self-propelling speed. All particles undergo rotational Brownian motion with a characteristic reorientation time τ_R , where the particle's orientation vector is restricted to the two-dimensional plane parallel to the channel. Thus, the motion of each particle is governed by the overdamped set of equations:

$$v = \dot{x} = \gamma^{-1}(F_a + F_c) = U_a \cos(\theta) + \gamma^{-1}F_c, \quad (1a)$$

$$\dot{\theta} = \xi(t), \quad (1b)$$

where F_c is the interparticle force and $\xi(t)$ is Gaussian white noise characterized by $\langle \xi(t) \rangle = 0$ and $\langle \xi(t)\xi(t') \rangle = (2/\tau_R)\delta(t-t')$. We consider the limit where the effects of translational Brownian motion are nominal. The interparticle force F_c arises from a Weeks-Chandler-Anderson (WCA) potential characterized by a potential depth ε and Lennard-Jones diameter σ [100]. As our active force is bounded, a sufficiently steep potential mimics a hard-particle interaction. A choice of $\varepsilon/(F_a\sigma) = 100$

results in hard particle statistics with a particle length of $\sigma_p = 2^{1/6}\sigma$. Using the HOOMD-blue software package [101], all simulations were conducted with 1,000 particles and run for a minimum duration of $5,000 \sigma/U_0$.

Two dimensionless parameters describe the state of the purely-repulsive 1D-ABP system: the packing fraction $\phi = \rho\sigma_p$ where $\rho = N/L$ is the particle line density and the dimensionless run-length $\ell_0 = (U_a\tau_R)/\sigma$. In the limit of small run-lengths, the behavior of the 1D-ABP system recovers that of the equilibrium Tonks gas. The emergent behavior that arises as run-length increases is the formation of large dynamic clusters. Cluster formation appears to be a universal feature of 1D active matter systems and has been previously observed in several studies [102–111]. To quantify cluster formation, we define an empirical measure of the degree of clustering $\Theta = 1 - 1/\langle N_c \rangle$, where $\langle N_c \rangle$ is the average number of particles in a cluster and $\langle \dots \rangle$ denotes a time average. Here, particles are considered clustered when in contact (i.e., the separation distance is less than σ_p). If there are predominately unclustered particles in the system $\Theta \approx 0$, while if all particles belong to a single cluster $\Theta = 1 - 1/N \approx 1$.

In Fig. 2(a), we plot the degree of clustering Θ for the 1D-ABP system as a function of packing fraction ϕ for different values of ℓ_0 . The degree of clustering increases with the packing fraction and approaches $\Theta = 1$ at close-packing (i.e., $\phi = 1$). In the opposite limit as $\phi \rightarrow 0$, there is little clustering and $\Theta \rightarrow 0$. Yet, it is notable that Θ can increase dramatically even at low packing fractions when ℓ_0 becomes large. In the Supplemental Material [112], we include movies from simulations illustrating the cluster dynamics at different run-lengths.

A notable observation for the 1D-ABP system is that particles’ velocities are significantly reduced when clustered. To quantify this reduction in particle speed, we define a reduced average translational kinetic energy: $\mathcal{K} = K/K_0 = 2\langle v^2 \rangle/U_a^2$, where K and K_0 are the kinetic energies of the interacting and ideal 1D-ABP system, respectively. It is worth noting the reduced average translation kinetic energy \mathcal{K} is closely related to the dissipation or irreversible energy loss typically defined in stochastic thermodynamics [113, 114]. Interestingly, recent work has linked dissipation to the structure and transport properties of active liquids [115–117].

For the 1D-ABP system, it is easy to show from Eq. (1) that $\mathcal{K} = 1 - 2\langle F_c^2 \rangle/(\gamma U_a)^2$. The second term represents the reduction in kinetic energy due to interparticle collisions. In deriving \mathcal{K} , we use a unique property of ABPs, which we prove in the Supplemental Material [112], where $\langle vF_c \rangle = 0$. A consequence of this property is $\langle F_a F_c \rangle = -\langle F_c^2 \rangle$ for all packing fractions, run-lengths, and system sizes. Remarkably, this property is not a result of 1D confinement, but the analog $\langle \mathbf{v} \cdot \mathbf{F}_c \rangle = 0$ is also true for ABPs in higher dimensions.

For a 1D system in thermal equilibrium, the temperature T can be obtained by application of the equiparti-

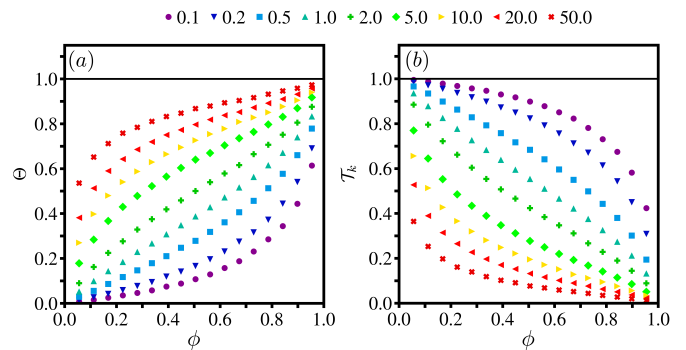


FIG. 2. (a) Degree of clustering Θ and (b) reduced kinetic temperature \mathcal{T}_k as a function of packing fraction ϕ for different run-lengths ℓ_0 .

tion theorem to give the well-known result $k_B T = 2K/N$, where k_B is the Boltzmann constant. In a similar spirit, we define a kinetic temperature for ABPs as $T_k = 2K/N$, resulting in a reduced kinetic temperature:

$$\mathcal{T}_k = \frac{T_k}{T_0} = 1 - \frac{2\langle F_c^2 \rangle}{(\gamma U_a)^2}, \quad (2)$$

where T_0 is the kinetic temperature of the ideal active system, and the second term is the relative reduction of the kinetic temperature due to collisions.

In Fig. 2(b), we plot \mathcal{T}_k for the 1D-ABP system. The reduced kinetic temperature decreases monotonically as the packing fraction increases and, in agreement with our previous observation, scales inversely with the degree of clustering shown in Fig 1(a). At low packing fraction, \mathcal{T}_k approaches the ideal result, and at close-packing, \mathcal{T}_k tends to zero for all run-lengths. This temperature reduction or kinetic energy loss is a peculiarity of active Brownian systems. The inelastic nature of collisions reduces a particle’s velocity during a collision and, in turn, temporarily removes kinetic energy from the system.

The utility of \mathcal{T}_k is that it can be related directly to the mechanical pressure. The total pressure for the 1D-ABP system is computed via the virial theorem as $P = \rho \langle x F_{net} \rangle$ where $F_{net} = F_a + F_c$ is the net force acting on a particle. Here, P is the average force the ABPs exert on the boundary. The two contributions to the total pressure P are the collisional pressure $P_c = \rho \langle x F_c \rangle$ and the swim pressure $P_s = \rho \langle x F_a \rangle$. For convenience, we use an alternative yet equivalent expression for the swim pressure valid for ABPs known as the “active impulse” form given by $P_s = \rho \langle v F_a \rangle \tau_R$ [118–120]. The pressure of the ideal 1D-ABP system is $P_0 = \rho \gamma U_a^2 \tau_R / 2$, and the reduced swim pressure of the interacting system is

$$\mathcal{P}_s = \frac{P_s}{P_0} = 1 - \frac{2\langle F_c^2 \rangle}{(\gamma U_a)^2}, \quad (3)$$

where we again use the relation $\langle F_a F_c \rangle = -\langle F_c^2 \rangle$. Upon comparison of Eq. (2) and Eq. (3), we find the two expressions are identical and arrive at one of the central results

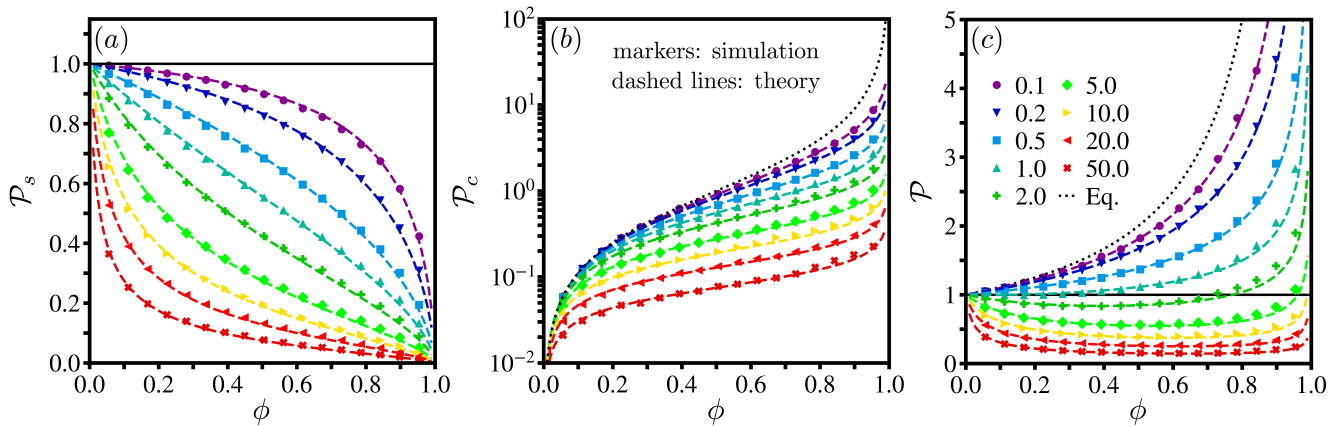


FIG. 3. Brownian dynamics simulation results for the reduced (a) swim pressure, (b) collisional pressure, and (c) total pressure as a function of packing fraction for different run-lengths. The dotted lines correspond to the analytical expressions for the Tonks gas. The dashed curves are the analytical expression derived based on the scaling argument for the kinetic temperature.

of this work, which is the equivalence of the reduced swim pressure and reduced kinetic temperature: $\mathcal{P}_s = \mathcal{T}_k$. This equivalence can be easily extended to ABPs in higher dimensions, as shown in the Supplemental Material [112]. In Fig. 3(a), we plot \mathcal{P}_s computed from simulation and validate $\mathcal{P}_s = \mathcal{T}_k$ by comparison with Fig. 2(b). A practical outcome of $\mathcal{P}_s = \mathcal{T}_k$ is that the kinetic temperature offers a convenient method of computing the swim pressure of ABPs as particle velocities are readily available from simulation.

We derive an analytical expression for the reduced kinetic temperature using a simple scaling argument predicated on the dynamics of an individual particle. There are two relevant timescales for a given particle: the average duration of a collision τ_C and the average time between collisions τ_F . The reduced kinetic temperature can be estimated as $\mathcal{T}_k = [(1)\tau_F + (0)\tau_C]/(\tau_F + \tau_C) = 1/(1 + \tau_C/\tau_F)$, where between collisions $\mathcal{T}_k = 1$ as particle motion is unimpeded and during a collision $\mathcal{T}_k = 0$. We approximate the duration of a collision as being comparable to the reorientation time of a particle: $\tau_C \sim \tau_R$. While the time between collision scales as $\tau_F \sim \lambda/U_a$, where λ is the mean free path and U_a is the intrinsic speed of a particle. The mean free path in the limit of small run-length is $\lambda = (1 - \phi)/\rho$ as particles are nearly uniformly distributed. For the more general case, $\lambda \sim (1 - \phi)/(\rho\sqrt{\mathcal{T}_k})$ as clustering increases the distance a particle must travel between collisions (see Supplemental Material [112]). A full discussion of the dependence of τ_C and τ_F will be published separately.

This expression captures the asymptotic behavior of the reduced kinetic temperature in Fig. 2(b) (i.e., $\mathcal{T}_k \rightarrow 1$ as $\tau_C/\tau_F \rightarrow 0$ and $\mathcal{T}_k \rightarrow 0$ as $\tau_C/\tau_F \rightarrow \infty$). We expect the exact value of the kinetic temperature will be sensitive to the assumption that particle velocities are exactly zero when clustered. We recognize this is not strictly true as we observe that clusters retain a small

drift velocity. To account for this drift behavior and the approximation of τ_C and τ_F , we introduce a correction factor α , to be determined *a posteriori*, and obtain an algebraic equation for the reduced kinetic temperature:

$$\mathcal{T}_k = \left(1 + \alpha \frac{\tau_C}{\tau_F}\right)^{-1} = \left(1 + \alpha \ell_0 \frac{\phi}{1 - \phi} \sqrt{\mathcal{T}_k}\right)^{-1}. \quad (4)$$

By solving Eq. (4) (see Supplemental Material [112]), we obtain the following analytical expression for \mathcal{T}_k :

$$\mathcal{T}_k = \frac{1}{9b^2} \left[2 \cos \left(\frac{1}{3} \arccos \left(\frac{27}{2} b^2 - 1 \right) \right) - 1 \right]^2, \quad (5)$$

where $b = \alpha \ell_0 \phi / (1 - \phi)$. In Fig. 3(a), we find excellent agreement between simulation results and our analytical solution for \mathcal{T}_k or equivalently \mathcal{P}_s . As expected, α exhibits a weak dependence on ℓ_0 and can be approximated by $\alpha = c/(1 + \ell_0)^d$ where $c = 1.1$ and $d = 0.05$.

We now derive an analytical expression for the collisional pressure of the 1D-ABP system. As the run-length decreases, the collisional pressure [Fig. 3(b)] approaches the known analytical result for the equilibrium system: $\mathcal{P}_c = P_c/P_0 = \phi/(1 - \phi)$. For particles interacting through an additive pairwise potential, the collisional pressure can be expressed as $P_c = \rho \langle x_{ij} F_{ij} \rangle / 2$ where $x_{ij} = x_j - x_i$ is the distance between the i^{th} and j^{th} particles and F_{ij} is the resulting force between the pair. As we consider nearly hard particle interactions, a suggestive scaling for the collisional pressure is $P_c = \rho \langle x_{ij} F_{ij} \rangle / 2 \sim \rho (\sigma_p \bar{F}_{ij}) / 2$, where \bar{F}_{ij} is the average magnitude of the force experienced between a pair of particle. To recover the equilibrium result in the limit of small run-lengths, it is required $\bar{F}_{ij} = \gamma U_a^2 \tau_R [\rho / (1 - \phi)] = \mathcal{F}_a \tau_C / \tau_F$, where $\mathcal{F}_a = \gamma U_a$. This expression for \bar{F}_{ij} can be generalized to large run-lengths by replacing the force scale \mathcal{F}_a by a more appropriate force scale $\mathcal{F}_a = \gamma U_a \sqrt{\mathcal{T}_k}$, which captures the observed reduction in \mathcal{P}_c as ℓ_0 is increased [see

trend in Fig. 3(b)]. Thus, an expression for P_c valid for all run-lengths is

$$P_c = \frac{\rho}{2} \left(\sigma_p \gamma U_a \sqrt{\mathcal{T}_k} \frac{\tau_C}{\tau_F} \right) = P_s \left[\frac{\phi}{1-\phi} \right]. \quad (6)$$

In Fig. 3(b), we see excellent agreement between simulation results and the analytical expression: $\mathcal{P}_c = \mathcal{T}_k[\phi/(1-\phi)]$. Remarkably, the reduced collisional pressure is simply the product of \mathcal{T}_k and the equilibrium collisional pressure of the Tonks gas. A unique feature of the 1D-ABP system, highlighted in Fig. 4(a), is the ratio of the collisional and swim pressure collapses onto a universal curve given by $P_c/P_s = \phi/(1-\phi)$. This behavior is a direct result of the single-file confinement and not observed for ABPs in higher dimensions [121–125].

By combining our results for the swim and collisional pressure, we achieve our primary aim of an analytical expression for the total pressure of the 1D-ABP system:

$$\mathcal{P} = \mathcal{P}_s + \mathcal{P}_c = \mathcal{T}_k \left[1 + \frac{\phi}{1-\phi} \right] = \mathcal{T}_k \left[\frac{1}{1-\phi} \right]. \quad (7)$$

In Fig. 3(c), we find excellent agreement between our analytical expression for \mathcal{P} and simulation results. In the limit of small run-lengths, Eq. (7) reproduces the analytical result for the equilibrium Tonks gas: $\mathcal{P} = 1/(1-\phi)$. We also identify an analog to the Boyle temperature of an equilibrium system, which we call the Boyle run-length, where the second virial coefficient is zero and $\mathcal{P} \approx 1$. The Boyle run-length occurs at $\ell_0 \approx 1$ and indicates a crossover from a regime where the interaction between particles are predominantly repulsive to one where there is an effective attraction between particles. This crossover is consistent with the activity-induced clustering shown in Fig. 2(a). It is straightforward to show from Eq. (7) that the single homogeneous phase for the 1D-ABP system is always mechanically stable (i.e. $(\partial P/\partial \rho)_{\ell_0} > 0$). These findings provide a mechanical interpretation to prior studies on 1D active systems where there was found to be clustering but no motility-induced phase separation [102–111].

We can further quantify the clustering behavior by investigating the constant run-length compressibility – a thermodynamic-like response function that provides a measure of clustering and local density fluctuations [126, 127]. In Fig. 4(b), the reduced constant run-length compressibility was calculated from Eq. (7) as

$$\mathcal{X} = \frac{\chi_a}{\chi_0} = \left[\frac{\mathcal{T}_k}{(1-\phi)^2} + \frac{\phi}{1-\phi} \left(\frac{\partial \mathcal{T}_k}{\partial \phi} \right) \right]^{-1}, \quad (8)$$

where $\chi_a = (\partial \ln \rho / \partial P)_{\ell_0}$ and $\chi_0 = 1/P_0$ are the compressibility for the interacting and ideal system, respectively. In the limit of small run-lengths, the 1D-ABP system approaches the result of the equilibrium Tonks gas $\mathcal{X} = (1-\phi)^2$ and in the ideal limit where $\phi \rightarrow 0$, $\mathcal{X} \rightarrow 1$.

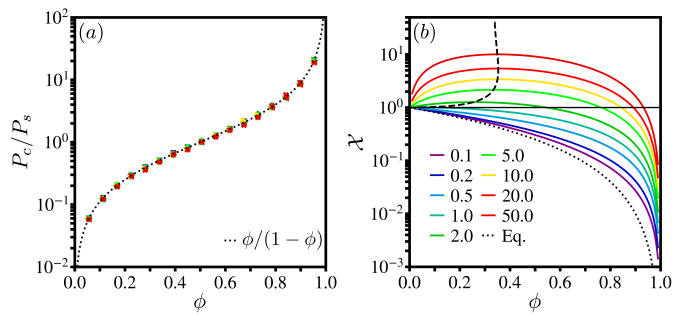


FIG. 4. The ratio of the collisional pressure P_c to the swim pressure P_s for the 1D-ABP system collapse onto a universal curve $P_c/P_s = \phi/(1-\phi)$. (b) The compressibility as a function of packing fraction for various run-lengths. The dotted line corresponds to the reduced compressibility of the equilibrium Tonks gas $\mathcal{X} = (1-\phi)^2$. The dashed line traces the location of the maximum of the reduced compressibility \mathcal{X}_m .

Above the Boyle run-length, \mathcal{X} is no longer monotonic but exhibits a maximum \mathcal{X}_m . The existence of this maximum suggests a structural transition or weak thermodynamic singularity similar to the Frenkel or Widom line of supercritical fluids [128–131] and will be characterized in future work.

In the limit of large run-length, the location of \mathcal{X}_m becomes independent of ℓ_0 and analytically can be shown to asymptotically approach a packing fraction $\phi = 1/3$ as shown by the dashed line in Fig. 4(b). For these large values of the run-length, \mathcal{X}_m exhibits a power law dependence given by $\mathcal{X}_m \approx 0.9(\ell_0)^{19/30}$. If we consider $\mathcal{X}/\mathcal{X}_m$ for these large run-lengths (See Supplemental Material [112]), we observe a collapse onto a universal curve similar in shape to that of $\ell_0 = 50$ in Fig. 4(b). The 1D-ABP system has the interesting property that the compressibility can be made arbitrarily large by increasing the run-length, but there is no emergent singularity consistent with a critical point as the shape of \mathcal{X} stops evolving in the limit of large run-lengths. A physical interpretation of this behavior is that density fluctuations and clusters can become arbitrarily large, but it is impossible to form a large stable cluster that would give rise to a new dense phase.

Conclusions.– This work derives an accurate analytical expression for the mechanical pressure of a purely-repulsive 1D-ABP system using the concept of kinetic temperature. By analyzing trends in the pressure, we obtain a mechanical interpretation for the phase behavior of the 1D-ABP system and the lack of a motility-induced phase transition. Further investigation is warranted to establish when the concept of a kinetic temperature can be extended to other active particle models, including those with hydrodynamic or electrostatic interactions.

Acknowledgments.– We thank Parvin Bayati, Yunhee Choi, Akin Akintunde, and Will Noid for helpful discussions and critically reading an early draft of the

manuscript.

* hrow@berkeley.edu

† sam7808@psu.edu

- [1] L. Tonks, The complete equation of state of one, two and Three-Dimensional gases of hard elastic spheres, *Phys. Rev.* **50**, 955 (1936).
- [2] R. L. Sells, C. W. Harris, and E. Guth, The pair distribution function for a One-Dimensional gas, *J. Chem. Phys.* **21**, 1422 (1953).
- [3] Z. W. Salsburg, R. W. Zwanzig, and J. G. Kirkwood, Molecular distribution functions in a One-Dimensional fluid, *J. Chem. Phys.* **21**, 1098 (1953).
- [4] D. Koppel, Partition function for a generalized tonks' gas, *Phys. Fluids* **6**, 609 (1963).
- [5] F. Gürsey, Classical statistical mechanics of a rectilinear assembly, *Math. Proc. Cambridge Philos. Soc.* **46**, 182 (1950).
- [6] G. S. Rushbrooke and H. D. Ursell, On one-dimensional regular assemblies, *Math. Proc. Cambridge Philos. Soc.* **44**, 263 (1948).
- [7] A. Santos, A concise course on the theory of classical liquids, *Lecture Notes in Physics* **923** (2016).
- [8] J.-P. Hansen and I. R. McDonald, *Theory of simple liquids: with applications to soft matter* (Academic press, 2013).
- [9] M. Kac, G. E. Uhlenbeck, and P. C. Hemmer, On the van der waals theory of the Vapor-Liquid equilibrium. i. discussion of a One-Dimensional model, *J. Math. Phys.* **4**, 216 (1963).
- [10] E. Helfand, H. L. Frisch, and J. L. Lebowitz, Theory of the two- and One-Dimensional rigid sphere fluids, *J. Chem. Phys.* **34**, 1037 (1961).
- [11] J. S. Rowlinson, The equation of state of dense systems, *Rep. Prog. Phys.* **28**, 169 (1965).
- [12] A. Robledo and J. S. Rowlinson, The distribution of hard rods on a line of finite length, *Mol. Phys.* **58**, 711 (1986).
- [13] F. C. Andrews, Simple approach to the equilibrium statistical mechanics of the hard sphere fluid, *J. Chem. Phys.* **62**, 272 (1975).
- [14] V. M. Pergamenschchik, Analytical canonical partition function of a quasi-one-dimensional system of hard disks, *J. Chem. Phys.* **153**, 144111 (2020).
- [15] A. Lenard, Exact statistical mechanics of a One-Dimensional system with coulomb forces, *J. Math. Phys.* **2**, 682 (1961).
- [16] F. Ceconi, F. Diotallevi, U. M. B. Marconi, and A. Puglisi, Fluid-like behavior of a one-dimensional granular gas, *J. Chem. Phys.* **120**, 35 (2004).
- [17] B. Lin, M. Meron, B. Cui, S. A. Rice, and H. Diamant, From random walk to single-file diffusion, *Phys. Rev. Lett.* **94**, 216001 (2005).
- [18] J. Liam McWhirter, H. Noguchi, and G. Gompper, Deformation and clustering of red blood cells in microcapillary flows, *Soft Matter* **7**, 10967 (2011).
- [19] E. Locatelli, M. Pierno, F. Baldovin, E. Orlandini, Y. Tan, and S. Pagliara, Single-File escape of colloidal particles from microfluidic channels, *Phys. Rev. Lett.* **117**, 038001 (2016).
- [20] C. Coste, J.-B. Delfau, C. Even, and M. Saint Jean, Single-file diffusion of macroscopic charged particles, *Phys. Rev. E Stat. Nonlin. Soft Matter Phys.* **81**, 051201 (2010).
- [21] M. M. Calbi, S. M. Gatica, and M. W. Cole, Statistical mechanics of interacting peapods, *Phys. Rev. B Condens. Matter* **67**, 205417 (2003).
- [22] H. Hansen-Goos, C. Lutz, C. Bechinger, and R. Roth, From pair correlations to pair interactions: An exact relation in one-dimensional systems, *EPL* **74**, 8 (2006).
- [23] C. Lutz, M. Kollmann, and C. Bechinger, Single-file diffusion of colloids in one-dimensional channels, *Phys. Rev. Lett.* **93**, 026001 (2004).
- [24] Q. Wei, C. Bechinger, and P. Leiderer, Single-file diffusion of colloids in one-dimensional channels, *Science* **287**, 625 (2000).
- [25] K. Misiunas and U. F. Keyser, Density-Dependent speed-up of particle transport in channels, *Phys. Rev. Lett.* **122**, 214501 (2019).
- [26] P. Romanczuk, M. Bär, W. Ebeling, B. Lindner, and L. Schimansky-Geier, Active brownian particles, *Eur. Phys. J. Spec. Top.* **202**, 1 (2012).
- [27] S. A. Mallory, C. Valeriani, and A. Cacciuto, An active approach to colloidal Self-Assembly, *Annu. Rev. Phys. Chem.* **69**, 59 (2018).
- [28] C. Bechinger, R. Di Leonardo, H. Löwen, C. Reichhardt, G. Volpe, and G. Volpe, Active particles in complex and crowded environments, *Rev. Mod. Phys.* **88**, 045006 (2016).
- [29] M. R. Shaebani, A. Wysocki, R. G. Winkler, G. Gompper, and H. Rieger, Computational models for active matter, *Nature Reviews Physics* **2**, 181 (2020).
- [30] G. Gompper, R. G. Winkler, T. Speck, A. Solon, C. Nardini, F. Peruani, H. Löwen, R. Golestanian, U. B. Kaupp, L. Alvarez, T. Kiørboe, E. Lauga, W. C. K. Poon, A. DeSimone, S. Muiños-Landin, A. Fischer, N. A. Söker, F. Cichos, R. Kapral, P. Gaspard, M. Ripoll, F. Sagues, A. Doostmohammadi, J. M. Yeomans, I. S. Aranson, C. Bechinger, H. Stark, C. K. Hemelrijk, F. J. Nedelec, T. Sarkar, T. Aryaksama, M. Lacroix, G. Duclos, V. Yashunsky, P. Silberzan, M. Arroyo, and S. Kale, The 2020 motile active matter roadmap, *J. Phys. Condens. Matter* **32**, 193001 (2020).
- [31] A. Zöttl and H. Stark, Modeling active colloids: From active brownian particles to hydrodynamic and chemical fields, *Annu. Rev. Condens. Matter Phys.* (2023).
- [32] J. Jeggle, J. Stenhammar, and R. Wittkowski, Pair-distribution function of active brownian spheres in two spatial dimensions: Simulation results and analytic representation, *J. Chem. Phys.* **152**, 194903 (2020).
- [33] J. Bickmann and R. Wittkowski, Collective dynamics of active brownian particles in three spatial dimensions: A predictive field theory, *Phys. Rev. Res.* **2**, 033241 (2020).
- [34] M. O. Din, T. Danino, A. Prindle, M. Skalak, J. Selimkhanov, K. Allen, E. Julio, E. Atolia, L. S. Tsimring, S. N. Bhatia, and J. Hasty, Synchronized cycles of bacterial lysis for in vivo delivery, *Nature* **536**, 81 (2016).
- [35] A. Ghosh, W. Xu, N. Gupta, and D. H. Gracias, Active matter therapeutics, *Nano Today* **31** (2020).
- [36] J. K. Patra, G. Das, L. F. Fraceto, E. V. R. Campos, M. D. P. Rodriguez-Torres, L. S. Acosta-Torres, L. A. Diaz-Torres, R. Grillo, M. K. Swamy, S. Sharma, S. Habtemariam, and H.-S. Shin, Nano based drug delivery systems: recent developments and future prospects,

- J. Nanobiotechnology **16**, 71 (2018).
- [37] M. Kumar, J. S. Guasto, and A. M. Ardekani, Transport of complex and active fluids in porous media, *J. Rheol.* **66**, 375 (2022).
- [38] T. Bhattacharjee, D. B. Amchin, J. A. Ott, F. Kratz, and S. S. Datta, Chemotactic migration of bacteria in porous media, *Biophys. J.* **120**, 3483 (2021).
- [39] W. Yan and J. F. Brady, The curved kinetic boundary layer of active matter, *Soft Matter* **14**, 279 (2018).
- [40] T. Jamali and A. Naji, Active fluids at circular boundaries: swim pressure and anomalous droplet ripening, *Soft Matter* **14**, 4820 (2018).
- [41] W. Yan and J. F. Brady, The force on a boundary in active matter, *J. Fluid Mech.* **785** (2015).
- [42] A. Duzgun and J. V. Selinger, Active brownian particles near straight or curved walls: Pressure and boundary layers, *Phys Rev E* **97**, 032606 (2018).
- [43] N. Razin, Entropy production of an active particle in a box, *Phys Rev E* **102**, 030103 (2020).
- [44] Y. Fily, A. Baskaran, and M. F. Hagan, Dynamics of self-propelled particles under strong confinement, *Soft Matter* **10**, 5609 (2014).
- [45] T. Ostapenko, F. J. Schwarzendahl, T. J. Bøddeker, C. T. Kreis, J. Cammann, M. G. Mazza, and O. Bäumchen, Curvature-Guided motility of microalgae in geometric confinement, *Phys. Rev. Lett.* **120**, 068002 (2018).
- [46] S. Das and A. Cacciuto, Colloidal swimmers near curved and structured walls, *Soft Matter* **15**, 8290 (2019).
- [47] F. Turci and N. B. Wilding, Wetting transition of active brownian particles on a thin membrane, *Phys. Rev. Lett.* **127**, 238002 (2021).
- [48] S. Ketzetzi, M. Rinaldin, P. Dröge, J. d. Graaf, and D. J. Kraft, Activity-induced interactions and cooperation of artificial microswimmers in one-dimensional environments, *Nat. Commun.* **13**, 1772 (2022).
- [49] R. G. Winkler, A. Wysocki, and G. Gompper, Virial pressure in systems of spherical active brownian particles, *Soft Matter* **11**, 6680 (2015).
- [50] S. A. Mallory, A. Sárić, C. Valeriani, and A. Cacciuto, Anomalous thermomechanical properties of a self-propelled colloidal fluid, *Phys. Rev. E Stat. Nonlin. Soft Matter Phys.* **89**, 052303 (2014).
- [51] A. P. Solon, J. Stenhammar, R. Wittkowski, M. Kardar, Y. Kafri, M. E. Cates, and J. Tailleur, Pressure and phase equilibria in interacting active brownian spheres, *Phys. Rev. Lett.* **114**, 198301 (2015).
- [52] S. C. Takatori, W. Yan, and J. F. Brady, Swim pressure: stress generation in active matter, *Phys. Rev. Lett.* **113**, 028103 (2014).
- [53] A. P. Solon, Y. Fily, A. Baskaran, M. E. Cates, Y. Kafri, M. Kardar, and J. Tailleur, Pressure is not a state function for generic active fluids, *Nat. Phys.* **11**, 673 (2015).
- [54] F. Smalenburg and H. Löwen, Swim pressure on walls with curves and corners, *Phys. Rev. E Stat. Nonlin. Soft Matter Phys.* **92**, 032304 (2015).
- [55] T. Speck and R. L. Jack, Ideal bulk pressure of active brownian particles, *Phys Rev E* **93**, 062605 (2016).
- [56] M. Joyeux and E. Bertin, Pressure of a gas of underdamped active dumbbells, *Phys Rev E* **93**, 032605 (2016).
- [57] U. Marini Bettolo Marconi, C. Maggi, and M. Paoluzzi, Pressure in an exactly solvable model of active fluid, *J. Chem. Phys.* **147**, 024903 (2017).
- [58] J. M. Epstein, K. Klymko, and K. K. Mandadapu, Statistical mechanics of transport processes in active fluids. II. equations of hydrodynamics for active brownian particles, *J. Chem. Phys.* **150**, 164111 (2019).
- [59] A. K. Omar, Z.-G. Wang, and J. F. Brady, Microscopic origins of the swim pressure and the anomalous surface tension of active matter, *Phys Rev E* **101**, 012604 (2020).
- [60] U. Marini Bettolo Marconi, C. Maggi, and S. Melchionna, Pressure and surface tension of an active simple liquid: a comparison between kinetic, mechanical and free-energy based approaches, *Soft Matter* **12**, 5727 (2016).
- [61] J. U. Klamsner, S. C. Kapfer, and W. Krauth, Thermodynamic phases in two-dimensional active matter, *Nat. Commun.* **9**, 5045 (2018).
- [62] J. O'Byrne, A. Solon, J. Tailleur, and Y. Zhao, An introduction to motility-induced phase separation, arXiv preprint arXiv:2112.03979 (2021).
- [63] A. K. Omar, H. Row, S. A. Mallory, and J. F. Brady, Mechanical theory of nonequilibrium coexistence and motility-induced phase separation, arXiv preprint arXiv:2211.12673 (2022).
- [64] S. A. Mallory, A. K. Omar, and J. F. Brady, Dynamic overlap concentration scale of active colloids, *Phys Rev E* **104**, 044612 (2021).
- [65] Y. Fily and M. C. Marchetti, Athermal phase separation of self-propelled particles with no alignment, *Phys. Rev. Lett.* **108**, 235702 (2012).
- [66] G. S. Redner, M. F. Hagan, and A. Baskaran, Structure and dynamics of a phase-separating active colloidal fluid, *Phys. Rev. Lett.* **110**, 055701 (2013).
- [67] R. Wittkowski, A. Tiribocchi, J. Stenhammar, R. J. Allen, D. Marenduzzo, and M. E. Cates, Scalar φ^4 field theory for active-particle phase separation, *Nat. Commun.* **5**, 4351 (2014).
- [68] S. C. Takatori and J. F. Brady, Towards a thermodynamics of active matter, *Phys. Rev. E Stat. Nonlin. Soft Matter Phys.* **91**, 032117 (2015).
- [69] A. P. Solon, J. Stenhammar, M. E. Cates, Y. Kafri, and J. Tailleur, Generalized thermodynamics of phase equilibria in scalar active matter, *Phys Rev E* **97**, 020602 (2018).
- [70] S. Paliwal, J. Rodenburg, R. van Roij, and M. Dijkstra, Chemical potential in active systems: predicting phase equilibrium from bulk equations of state?, *New J. Phys.* **20**, 015003 (2018).
- [71] S. Hermann, D. de las Heras, and M. Schmidt, Phase separation of active brownian particles in two dimensions: anything for a quiet life, *Mol. Phys.* **119**, e1902585 (2021).
- [72] T. Speck, Coexistence of active brownian disks: van der waals theory and analytical results, *Phys Rev E* **103**, 012607 (2021).
- [73] H. R. Vutukuri, M. Hoore, C. Abaurrea-Velasco, L. van Buren, A. Dutto, T. Auth, D. A. Fedosov, G. Gompper, and J. Vermant, Active particles induce large shape deformations in giant lipid vesicles, *Nature* **586**, 52 (2020).
- [74] C. Wang, Y.-K. Guo, W.-d. Tian, and K. Chen, Shape transformation and manipulation of a vesicle by active particles, *J. Chem. Phys.* **150**, 044907 (2019).
- [75] M. C. Gandikota and A. Cacciuto, Rectification of confined soft vesicles containing active particles, *Soft Matter* **19**, 315 (2023).

- [76] P. Iyer, G. Gompper, and D. A. Fedosov, Non-equilibrium shapes and dynamics of active vesicles, *Soft Matter* **18**, 6868 (2022).
- [77] A. Sokolov, L. D. Rubio, J. F. Brady, and I. S. Aranson, Instability of expanding bacterial droplets, *Nat. Commun.* **9**, 1322 (2018).
- [78] S. C. Takatori and A. Sahu, Active contact forces drive nonequilibrium fluctuations in membrane vesicles, *Phys. Rev. Lett.* **124**, 158102 (2020).
- [79] K. Xie, B. Gorin, R. T. Cerbus, L. Alvarez, J.-M. Rampoux, and H. Kellay, Activity induced rigidity of liquid droplets, *Phys. Rev. Lett.* **129**, 138001 (2022).
- [80] L. Angelani, Spontaneous assembly of colloidal vesicles driven by active swimmers, *J. Phys. Condens. Matter* **31**, 075101 (2019).
- [81] P. Liu, S. Ye, F. Ye, K. Chen, and M. Yang, Constraint dependence of active depletion forces on passive particles, *Phys. Rev. Lett.* **124**, 158001 (2020).
- [82] Y. Baek, A. P. Solon, X. Xu, N. Nikola, and Y. Kafri, Generic Long-Range interactions between passive bodies in an active fluid, *Phys. Rev. Lett.* **120**, 058002 (2018).
- [83] J. Harder, S. A. Mallory, C. Tung, C. Valeriani, and A. Cacciuto, The role of particle shape in active depletion, *J. Chem. Phys.* **141**, 194901 (2014).
- [84] F. Feng, T. Lei, and N. Zhao, Tunable depletion force in active and crowded environments, *Phys Rev E* **103**, 022604 (2021).
- [85] L. Li, P. Liu, K. Chen, N. Zheng, and M. Yang, Active depletion torque between two passive rods, *Soft Matter* **18**, 4265 (2022).
- [86] M. Zaeifi Yamchi and A. Naji, Effective interactions between inclusions in an active bath, *J. Chem. Phys.* **147**, 194901 (2017).
- [87] R. Ni, M. A. Cohen Stuart, and P. G. Bolhuis, Tunable long range forces mediated by self-propelled colloidal hard spheres, *Phys. Rev. Lett.* **114**, 018302 (2015).
- [88] S. A. Mallory, C. Valeriani, and A. Cacciuto, Curvature-induced activation of a passive tracer in an active bath, *Phys. Rev. E Stat. Nonlin. Soft Matter Phys.* **90**, 032309 (2014).
- [89] S. A. Mallory, C. Valeriani, and A. Cacciuto, Anomalous dynamics of an elastic membrane in an active fluid, *Phys. Rev. E Stat. Nonlin. Soft Matter Phys.* **92**, 012314 (2015).
- [90] M. C. Gandikota and A. Cacciuto, Effective forces between active polymers, *Phys Rev E* **105**, 034503 (2022).
- [91] N. Nikola, A. P. Solon, Y. Kafri, M. Kardar, J. Tailleur, and R. Voituriez, Active particles with soft and curved walls: Equation of state, ratchets, and instabilities, *Phys. Rev. Lett.* **117**, 098001 (2016).
- [92] J. Harder, C. Valeriani, and A. Cacciuto, Activity-induced collapse and reexpansion of rigid polymers, *Phys. Rev. E Stat. Nonlin. Soft Matter Phys.* **90**, 062312 (2014).
- [93] S. A. Mallory, M. L. Bowers, and A. Cacciuto, Universal reshaping of arrested colloidal gels via active doping, *J. Chem. Phys.* **153**, 084901 (2020).
- [94] M. E. Szakasits, W. Zhang, and M. J. Solomon, Dynamics of fractal cluster gels with embedded active colloids, *Phys. Rev. Lett.* **119**, 058001 (2017).
- [95] A. K. Omar, Y. Wu, Z.-G. Wang, and J. F. Brady, Swimming to stability: Structural and dynamical control via active doping, *ACS Nano* **13**, 560 (2019).
- [96] A. Kaiser and H. Löwen, Unusual swelling of a polymer in a bacterial bath, *J. Chem. Phys.* **141**, 044903 (2014).
- [97] Y.-Q. Xia, W.-d. Tian, K. Chen, and Y.-Q. Ma, Globule-stretch transition of a self-attracting chain in the repulsive active particle bath, *Phys. Chem. Chem. Phys.* **21**, 4487 (2019).
- [98] M. E. Szakasits, K. T. Saud, X. Mao, and M. J. Solomon, Rheological implications of embedded active matter in colloidal gels, *Soft Matter* **15**, 8012 (2019).
- [99] K. T. Saud, M. Ganesan, and M. J. Solomon, Yield stress behavior of colloidal gels with embedded active particles, *J. Rheol.* **65**, 225 (2021).
- [100] J. D. Weeks, D. Chandler, and H. C. Andersen, Role of repulsive forces in determining the equilibrium structure of simple liquids, *J. Chem. Phys.* **54**, 5237 (1971).
- [101] J. A. Anderson, J. Glaser, and S. C. Glotzer, HOOMD-blue: A python package for high-performance molecular dynamics and hard particle monte carlo simulations, *Comput. Mater. Sci.* **173**, 109363 (2020).
- [102] E. Locatelli, F. Baldovin, E. Orlandini, and M. Pierno, Active brownian particles escaping a channel in single file, *Phys. Rev. E Stat. Nonlin. Soft Matter Phys.* **91**, 022109 (2015).
- [103] P. Dolai, A. Das, A. Kundu, C. Dasgupta, A. Dhar, and K. V. Kumar, Universal scaling in active single-file dynamics, *Soft Matter* **16**, 7077 (2020).
- [104] P. de Castro, F. M. Rocha, S. Diles, R. Soto, and P. Sollich, Diversity of self-propulsion speeds reduces motility-induced clustering in confined active matter, *Soft Matter* **17**, 9926 (2021).
- [105] C. M. B. Gutiérrez, C. Vanhille-Campos, F. Alarcón, I. Pagonabarraga, R. Brito, and C. Valeriani, Collective motion of run-and-tumble repulsive and attractive particles in one-dimensional systems, *Soft Matter* **17**, 10479 (2021).
- [106] N. Sepúlveda and R. Soto, Universality of active wetting transitions, *Phys. Rev. E* **98**, 052141 (2018).
- [107] R. Soto and R. Golestanian, Run-and-tumble dynamics in a crowded environment: persistent exclusion process for swimmers, *Phys. Rev. E Stat. Nonlin. Soft Matter Phys.* **89**, 012706 (2014).
- [108] N. Sepúlveda and R. Soto, Coarsening and clustering in run-and-tumble dynamics with short-range exclusion, *Phys Rev E* **94**, 022603 (2016).
- [109] A. B. Slowman, M. R. Evans, and R. A. Blythe, Jamming and attraction of interacting Run-and-Tumble random walkers, *Phys. Rev. Lett.* **116**, 218101 (2016).
- [110] L. Caprini and U. Marini Bettolo Marconi, Active particles under confinement and effective force generation among surfaces, *Soft Matter* **14**, 9044 (2018).
- [111] I. Mukherjee, A. Raghu, and P. Mohanty, Nonexistence of motility induced phase separation transition in one dimension, arXiv preprint arXiv:2208.05937 (2022).
- [112] See Supplemental Material at [URL] for proof of $\langle vF_c \rangle = 0$ for the Active Brownian Particle System, the proof of $\mathcal{T}_k = \mathcal{P}_s$ for ABPs in higher dimensions, the estimation of the run-length dependence of the mean free path, additional details for solving the analytical expression for kinetic temperature, the large run-length behavior of the maximum constant-run-length-compressibility, and movies illustrating clustering dynamics at different run-lengths.
- [113] K. Sekimoto, Langevin equation and thermodynamics, *Progr. Theoret. Phys.* **130**, 17 (1998).

- [114] U. Seifert, Stochastic thermodynamics, fluctuation theorems and molecular machines, *Rep. Prog. Phys.* **75**, 126001 (2012).
- [115] G. Rassolov, L. Tociu, É. Fodor, and S. Vaikuntanathan, From predicting to learning dissipation from pair correlations of active liquids, *J. Chem. Phys.* **157**, 054901 (2022).
- [116] C. Del Junco, L. Tociu, and S. Vaikuntanathan, Energy dissipation and fluctuations in a driven liquid, *Proc. Natl. Acad. Sci. U. S. A.* **115**, 3569 (2018).
- [117] L. Tociu, É. Fodor, T. Nemoto, and S. Vaikuntanathan, How dissipation constrains fluctuations in nonequilibrium liquids: Diffusion, structure, and biased interactions, *Phys. Rev. X* **9**, 041026 (2019).
- [118] A. Patch, D. M. Sussman, D. Yllanes, and M. C. Marchetti, Curvature-dependent tension and tangential flows at the interface of motility-induced phases, *Soft Matter* **14**, 7435 (2018).
- [119] Y. Fily, Y. Kafri, A. P. Solon, J. Tailleur, and A. Turner, Mechanical pressure and momentum conservation in dry active matter, *J. Phys. A.* **51**, 044003 (2017).
- [120] S. Das, G. Gompper, and R. G. Winkler, Local stress and pressure in an inhomogeneous system of spherical active brownian particles, *Sci. Rep.* **9**, 6608 (2019).
- [121] A. K. Omar, K. Klymko, T. GrandPre, and P. L. Geissler, Phase diagram of active brownian spheres: Crystallization and the metastability of Motility-Induced phase separation, *Phys. Rev. Lett.* **126**, 188002 (2021).
- [122] T. Arnoulx de Pirey, G. Lozano, and F. van Wijland, Active hard spheres in infinitely many dimensions, *Phys. Rev. Lett.* **123**, 260602 (2019).
- [123] R. Dey, C. M. Buness, B. V. Hokmabad, C. Jin, and C. C. Maass, Oscillatory rheotaxis of artificial swimmers in microchannels, *Nat. Commun.* **13**, 2952 (2022).
- [124] P. Digregorio, D. Levis, A. Suma, L. F. Cugliandolo, G. Gonnella, and I. Pagonabarraga, Full phase diagram of active brownian disks: From melting to Motility-Induced phase separation, *Phys. Rev. Lett.* **121**, 098003 (2018).
- [125] D. Levis, J. Codina, and I. Pagonabarraga, Active brownian equation of state: metastability and phase coexistence, *Soft Matter* **13**, 8113 (2017).
- [126] A. R. Dulaney, S. A. Mallory, and J. F. Brady, The “isothermal” compressibility of active matter, *J. Chem. Phys.* **154**, 014902 (2021).
- [127] S. Chakraborti, S. Mishra, and P. Pradhan, Additivity, density fluctuations, and nonequilibrium thermodynamics for active brownian particles, *Phys Rev E* **93**, 052606 (2016).
- [128] D. Bolmatov, V. V. Brazhkin, and K. Trachenko, Thermodynamic behaviour of supercritical matter, *Nat. Commun.* **4**, 2331 (2013).
- [129] P. F. McMillan and H. E. Stanley, Going supercritical, *Nat. Phys.* **6**, 479 (2010).
- [130] G. G. Simeoni, T. Bryk, F. A. Gorelli, M. Krisch, G. Ruocco, M. Santoro, and T. Scopigno, The widom line as the crossover between liquid-like and gas-like behaviour in supercritical fluids, *Nat. Phys.* **6**, 503 (2010).
- [131] L. Xu, P. Kumar, S. V. Buldyrev, S.-H. Chen, P. H. Poole, F. Sciortino, and H. E. Stanley, Relation between the widom line and the dynamic crossover in systems with a liquid-liquid phase transition, *Proc. Natl. Acad. Sci. U. S. A.* **102**, 16558 (2005).

Supplemental Material: Kinetic temperature and pressure of an active Tonks gas

Elijah Schiltz-Rouse,¹ Hyeonjoo Row,^{2,*} and Stewart A. Mallory^{1,†}

¹*Department of Chemistry, The Pennsylvania State University, University Park, Pennsylvania, 16802, USA*

²*Department of Chemical and Biomolecular Engineering, UC Berkeley, Berkeley, CA 94720, USA*

(Dated: January 9, 2024)

PROOF OF $\langle vF_c \rangle = 0$ FOR ACTIVE BROWNIAN PARTICLES

We first present a simple cluster decomposition scheme to prove $\langle vF_c \rangle = 0$ for the one-dimensional active Brownian particle (ABP) system. The static correlation function of the velocity and collisional force at steady-state is defined as $\langle vF_c \rangle = \langle \sum_{i=1}^N v_i F_{c,i} \rangle / N$, where v_i and $F_{c,i}$ are the velocity and collisional force of the i^{th} particle, respectively, and N is the total number of particles. We rewrite the summation over individual particles as a sum over clusters:

$$\langle vF_c \rangle = \frac{1}{N} \left\langle \sum_{i=1}^{N_{\text{cl}}} \sum_{j \in \mathcal{C}_i} v_j F_{c,j} \right\rangle, \quad (\text{S1})$$

where N_{cl} is the number of clusters and \mathcal{C}_i is the set of indices of particles that form the i^{th} cluster. Here, particles are considered to be clustered when the separation distance is less than σ_p , where $\sigma_p = 2^{1/6}\sigma$ is the effective hard particle length, and σ is the standard Lennard-Jones diameter. Due to the inelastic nature of collisions, all particles within a cluster move at the same cluster velocity v^{cl} . Since particle interactions are short-ranged and conservative, the sum of interparticle forces within any cluster vanishes. Consequently, we obtain

$$\langle vF_c \rangle = \frac{1}{N} \left\langle \sum_{i=1}^{N_{\text{cl}}} v_i^{\text{cl}} \sum_{j \in \mathcal{C}_i} F_{c,j} \right\rangle = 0. \quad (\text{S2})$$

We highlight that Eq. (S2) combined with the equation of motion $v = (F_a + F_c)/\gamma$ results in $\langle F_a F_c \rangle = -\langle F_c^2 \rangle$, which establishes a bridge between the reduced kinetic temperature and reduced swim pressure as shown in the following section. Interestingly, this property is not a result of 1D confinement, but the analog $\langle \mathbf{v} \cdot \mathbf{F}_c \rangle = 0$ is also true for ABPs in higher dimensions. To prove this, we start from the fact that the rate of work performed by the active force is balanced by the rate of dissipation at steady-state: $\langle \mathbf{F}_a \cdot \mathbf{v} \rangle = \langle \gamma \mathbf{v} \cdot \mathbf{v} \rangle$ (see Ref. [1] for derivation). By substituting the velocity given by the equation of motion $\mathbf{v} = (\mathbf{F}_a + \mathbf{F}_c)/\gamma$ into the prior expression, we obtain $\langle \mathbf{v} \cdot \mathbf{F}_c \rangle = 0$.

PROOF OF $\mathcal{T}_k = \mathcal{P}_s$ FOR ABPS IN HIGHER DIMENSIONS

In the main text, we prove the equivalence of $\mathcal{T}_k = \mathcal{P}_s$ for ABPs in a single spatial dimension where particles have a single rotational degree of freedom. For a system with higher spatial dimensions $n_S \in \{2, 3\}$ containing active Brownian particles with n_R rotational degrees of freedom ($n_S - 1 \leq n_R \leq 2$), the swim pressure can be written as $\mathcal{P}_s = \rho \langle \mathbf{v} \cdot \mathbf{F}_a \rangle \tau_R / (n_S n_R)$. It follows the swim pressure for the ideal system is $P_0 = \rho \langle \mathbf{F}_a \cdot \mathbf{F}_a \rangle \tau_R / (n_S n_R \gamma)$ and the reduced swim pressure is

$$\mathcal{P}_s = \frac{P_s}{P_0} = 1 - \frac{n_R + 1}{n_S} \frac{\langle \mathbf{F}_c \cdot \mathbf{F}_c \rangle}{(\gamma U_a)^2}, \quad (\text{S3})$$

where we have used $\langle \mathbf{F}_a \cdot \mathbf{F}_c \rangle = -\langle \mathbf{F}_c \cdot \mathbf{F}_c \rangle$ and $\langle \mathbf{F}_a \cdot \mathbf{F}_a \rangle = n_S \gamma^2 U_a^2 / (n_R + 1)$. The average translational kinetic energy per particle is $K = m \langle \mathbf{v} \cdot \mathbf{v} \rangle / 2$ and for the ideal system $K_0 = m \langle \mathbf{F}_a \cdot \mathbf{F}_a \rangle / (2\gamma^2) = mn_S U_a^2 / (2(n_R + 1))$. Thus the reduced kinetic energy is

$$\mathcal{K} = \frac{K}{K_0} = 1 - \frac{n_R + 1}{n_S} \frac{\langle \mathbf{F}_c \cdot \mathbf{F}_c \rangle}{(\gamma U_a)^2}. \quad (\text{S4})$$

The kinetic temperature in n_S spatial dimensions is given by $T_k = 2K/n_s$, and it is straightforward to see $\mathcal{T}_k = \mathcal{K}$. Thus, $\mathcal{T}_k = \mathcal{P}_s$ for the more general case of ABPs in two and three dimensions.

ESTIMATION OF THE RUN-LENGTH DEPENDENCE OF THE MEAN FREE PATH

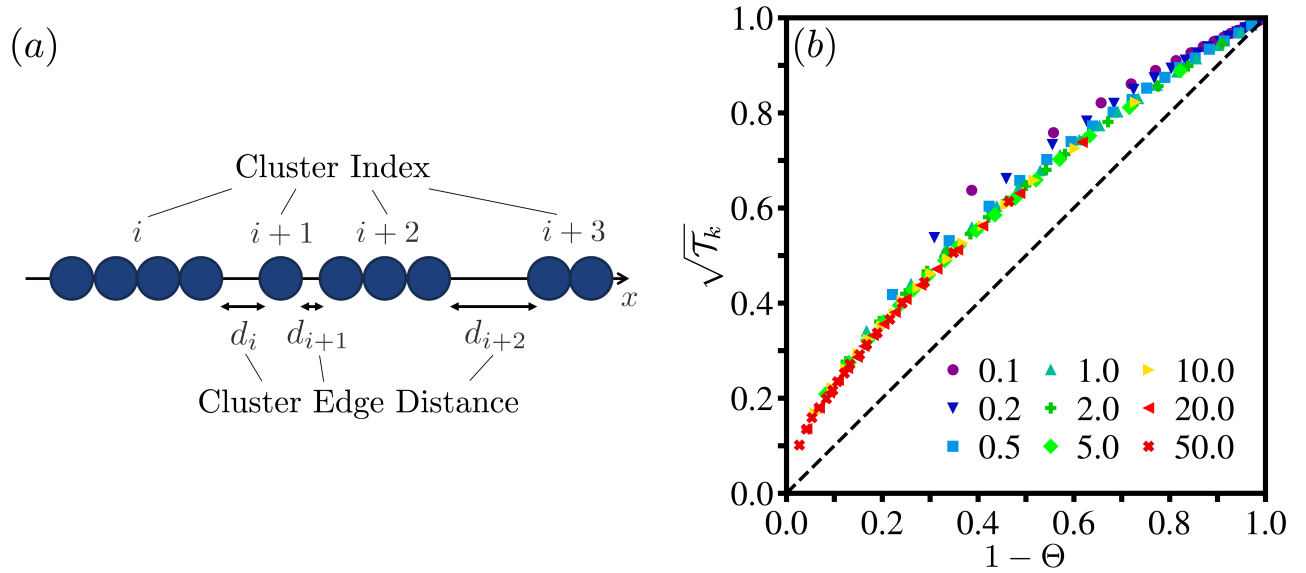


FIG. S1. (a) Schematic of 1D-ABP system illustrating the edge distance between clusters used to approximate the mean free path. Our scheme for enumerating clusters and the corresponding edge distances are shown above. (b) The relationship between $(1 - \Theta)$ and $\sqrt{\mathcal{T}_k}$ exhibit an approximately linear dependence, which was used in the final step of deriving the scaling for the mean free path [Eq. (S8)].

Our derivation of the reduced kinetic temperature \mathcal{T}_k (Eq. (4) of the main text) requires an estimate of the time between collision for an individual particle τ_F . We can express the time between collisions as $\tau_F = \lambda/U_a$ where U_a is the intrinsic speed of an ABP and λ is the mean free path. We estimate the mean free path as the average distance between the edges of any two adjacent clusters $\langle d \rangle$:

$$\lambda = \langle d \rangle = \left\langle \frac{1}{N_{\text{cl}}} \sum_{i=1}^{N_{\text{cl}}} d_i \right\rangle, \quad (\text{S5})$$

where d_i is the edge distance between the i^{th} and $(i+1)^{\text{th}}$ cluster (See Fig. S1(a)) and N_{cl} is the total number of clusters in a given configuration. As the system is periodic, we define $d_{N_{\text{cl}}}$ as the distance between the farthest right cluster and the first positive periodic image of the first cluster. The sum of all cluster edge distances is the total length that is not occupied by the particles (i.e., $\sum d_i = L - N\sigma_p$, where L is the length of the system, N is the number of particles, and σ_p is the diameter of a particle). Consequently, Eq. (S5) can be rewritten as

$$\lambda = \langle N_c \rangle \frac{1 - \phi}{\rho}, \quad (\text{S6})$$

where $\rho = N/L$ is the particle line density, $\phi = \rho\sigma_p$ is the packing fraction, and $\langle N_c \rangle$ is the average number of particles in a cluster. It follows from our definition for the degree of clustering $\Theta = 1 - 1/\langle N_c \rangle$, we can express the mean free path as

$$\lambda = \frac{1}{1 - \Theta} \frac{1 - \phi}{\rho}. \quad (\text{S7})$$

As noted in the main text, there exists an inverse relationship between reduced kinetic temperature \mathcal{T}_k and the degree of clustering Θ (See Fig. 2 of main text). It follows that $(1 - \Theta) \sim \mathcal{T}_k^\beta$ where β is a positive value. In Fig. S1(b), we plot $1 - \Theta$ versus $\sqrt{\mathcal{T}_k}$ and demonstrate an approximate linear scaling between the two quantities. Thus, an approximate scaling for the mean free path that captures the effects of clustering and increases with increasing run-length is

$$\lambda \sim \frac{1}{\sqrt{\mathcal{T}_k}} \frac{1 - \phi}{\rho}. \quad (\text{S8})$$

ANALYTICAL EXPRESSION FOR KINETIC TEMPERATURE

Equation (4) of the main text gives the algebraic equation for the kinetic temperature:

$$\mathcal{T}_k = \frac{1}{1 + \alpha \ell_0 \frac{\phi}{1-\phi} \sqrt{\mathcal{T}_k}} = \frac{1}{1 + b\sqrt{\mathcal{T}_k}}, \quad (\text{S9})$$

where $b = \alpha \ell_0 \phi / (1 - \phi)$, is introduced to write Eq. (S9) more compactly. A solution to Eq. (S9) can be obtained by using a substitution of variables $x = \sqrt{\mathcal{T}_k}$ to transform Eq. (S9) into a cubic equation: $bx^3 + x^2 - 1 = 0$. It is straightforward to rewrite this cubic expression as a depressed cubic and use Viète's formula to obtain:

$$\mathcal{T}_k = \frac{1}{9b^2} \left[2 \cos \left(\frac{1}{3} \arccos \left(\frac{27}{2} b^2 - 1 \right) \right) - 1 \right]^2. \quad (\text{S10})$$

**LARGE RUN-LENGTH BEHAVIOR OF THE MAXIMUM
CONSTANT-RUN-LENGTH-COMPRESSIBILITY**

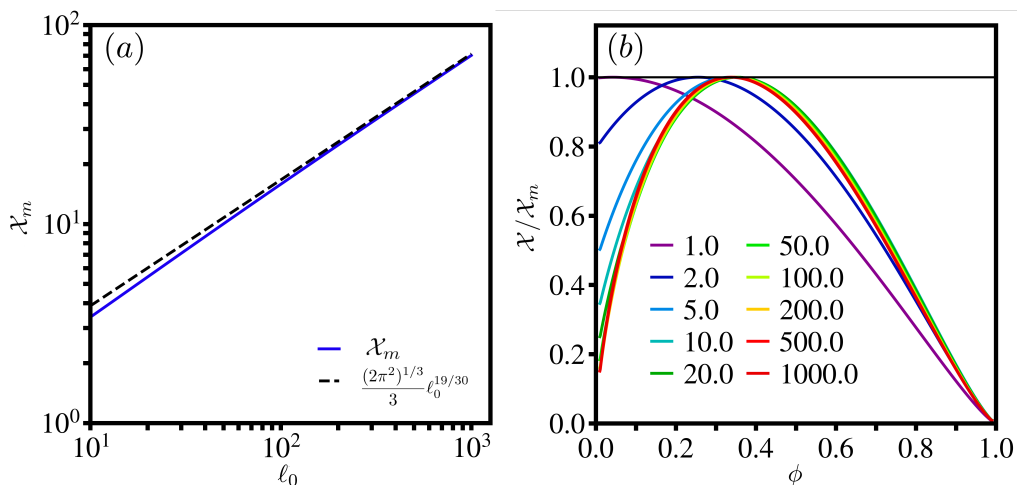


FIG. S2. (a) The run-length dependence of the maximum in the reduced constant-run-length compressibility \mathcal{X}_m , which scales as $\mathcal{X}_m = a(\ell_0)^{19/30}$ with $a = (2\pi^2)^{1/3}/3$ for large run-lengths. (b) The reduced constant run-length compressibility \mathcal{X} rescaled by the maximum \mathcal{X}_m , wherein the limit of large run-length the profile of $\mathcal{X}/\mathcal{X}_m$ takes on a constant profile shape.

In the main text we consider the reduced constant run-length compressibility \mathcal{X} (see Eq. (8) in the main text) to quantify the clustering behavior and present that \mathcal{X} admits a maximum value \mathcal{X}_m at sufficiently high run-lengths. Here, we perform a perturbative analysis on \mathcal{X}_m and present its asymptotic scaling behavior at high run-lengths $\ell_0 \gg 1$. From the equation of state (S10) with a parameter $\alpha = \pi(1 + \ell_0)^{-0.05}/2^{3/2}$ computed by simulation results, in the limit of $\ell_0 \rightarrow \infty$, \mathcal{X} is maximized when

$$3\pi^{\frac{2}{3}} \phi^{\frac{8}{3}} \left(\phi - \frac{1}{3} \right) + 4\phi^2 \left(\phi - \frac{2}{3} \right) (\phi - 1)^{\frac{2}{3}} \ell_0^{-\frac{19}{30}} + \mathcal{O} \left(\ell_0^{-\frac{19}{15}} \right) = 0. \quad (\text{S11})$$

Thus, the density ϕ_m at which a maximum value \mathcal{X}_m is attained approaches $1/3$ as activity increases. To determine the leading order behavior in the limit of $\ell_0 \rightarrow \infty$, we pose a perturbative expansion $\phi_m = 1/3 + c\ell_0^{-19/30} + \mathcal{O}(\ell_0^{-19/15})$. From the maximum condition (S11) with the expansion, we obtain the leading order coefficient $c = 4(2/\pi)^{2/3}/9$. By considering \mathcal{X} at ϕ_m we find the leading order behavior $\mathcal{X}_m = (2\pi^2)^{1/3} \ell_0^{19/30} / 3 + \mathcal{O}(1)$ as $\ell_0 \rightarrow \infty$.

DETAILS OF SIMULATION VIDEOS

Videos of typical trajectories illustrating the clustering dynamics for different values of the volume fraction ϕ and run-length ℓ_0 . Each particle has a vector representing its orientation and the coloring is based on cluster size. Note that only a portion of the system is visible in each video as it would be difficult to see the entire system otherwise. Videos are available at : [10.6084/m9.figshare.24461047](https://doi.org/10.6084/m9.figshare.24461047)

1. `video_1.mp4` - $\phi = 0.28$ and $\ell_0 = 0.1$
2. `video_2.mp4` - $\phi = 0.28$ and $\ell_0 = 1.0$
3. `video_3.mp4` - $\phi = 0.28$ and $\ell_0 = 10.0$
4. `video_4.mp4` - $\phi = 0.56$ and $\ell_0 = 0.1$
5. `video_5.mp4` - $\phi = 0.56$ and $\ell_0 = 1.0$
6. `video_6.mp4` - $\phi = 0.56$ and $\ell_0 = 10.0$
7. `video_7.mp4` - $\phi = 0.84$ and $\ell_0 = 0.1$
8. `video_8.mp4` - $\phi = 0.84$ and $\ell_0 = 1.0$
9. `video_9.mp4` - $\phi = 0.84$ and $\ell_0 = 10.0$

* hrow@berkeley.edu

† sam7808@psu.edu

- [1] A. K. Omar, K. Klymko, T. GrandPre, P. L. Geissler, and J. F. Brady, Tuning nonequilibrium phase transitions with inertia, *J. Chem. Phys.* **158**, 074904 (2023).